Environ. Sci. Technol. **1997**, *31*, 321−326

# Arsenate and Chromate Retention Mechanisms on Goethite. 2. Kinetic Evaluation Using a Pressure-Jump Relaxation Technique

PAUL R. GROSSL,*,† MATTHEW EICK,‡ DONALD L. SPARKS,§ SABINE GOLDBERG,|| AND CALVIN C. AINSWORTH⊥

*Department of Plants, Soils, and Biometeorology, Utah State University, Logan, Utah 84322-4820, Department of Agronomy, Louisiana Agricultural Experiment Station, Louisiana State University Agricultural Center, Baton Rouge, Louisiana 70803-2110, Department of Plant and Soil Sciences, University of Delaware, Newark, Delaware 19717-1303, USDA-ARS, U.S. Salinity Laboratory, 450 Big Springs Road, Riverside, California 92507, and Battelle, Pacific Northwest Laboratory, Richland, Washington 99352*

The kinetics of arsenate and chromate adsorption/desorption on goethite (α-FeOOH) were investigated using a pressure-jump (*p*-jump) relaxation technique. Information provided by this technique was used to elucidate the fate of arsenate and chromate in natural environments. Chemical relaxations resulting from rapidly induced pressure changes were monitored via conductivity detection. The adsorption/desorption of these oxyanions on goethite involved a double relaxation event. The proposed mechanism for the adsorption of arsenate and chromate on goethite is a two-step process resulting in the formation of an inner-sphere bidentate surface complex. The first step, associated with the fast $\tau$ values, involved an initial ligand exchange reaction of aqueous oxyanion species $H_2AsO_4^-$ or $HCrO_4^-$ with OH ligands at the goethite surface forming an inner-sphere monodentate surface complex. The subsequent step, associated with the slow $\tau$ values, involved a second ligand exchange reaction, resulting in the formation of an inner-sphere bidentate surface complex. Overall, the results suggest that chromate may be the more mobile of the two oxyanions in soil systems.

## Introduction

The accumulation of arsenate and chromate in soils and sediments threatens the health of plants, wildlife, and ultimately humans. Sources of contamination are predominately from human activities, arising from the disposal of industrial wastes, sewage sludges, mining and smelting operations, and agricultural chemicals. The potential of groundwater and surface water contamination by these pollutants has generated public and political concern, demanding swift and proper remediation of contaminated sites. However, proper cleanup and disposal requires an understanding of the fate of these oxyanions in soil environments.

In the redox range of most soil environments, arsenic can be found either as As(III) or As(V), and chromium as Cr(III) or Cr(VI). Under oxidizing conditions, arsenate (As(V)) and chromate (Cr(VI)) predominate. Soil solution levels of arsenate and chromate are governed by sorption processes, especially by adsorption onto the surfaces of iron oxides and hydroxides (*1*−*3*). The adsorption of both arsenate and chromate on iron oxides decreases with increasing pH and is a result of protonation of surface hydroxyl sites and the aqueous hydrolysis species of the oxyanions. Arsenate is specifically adsorbed, forming inner-sphere surface complexes with iron oxide surfaces (*1*−*3*) that are predominately bidentate (*2*−*4*). However, the nature of the surface complex (e.g., inner- or outer-sphere) that chromate forms with iron oxides has not been completely resolved. Indirect evidence suggests that the chromate/iron oxide surface complex is outer-sphere (*5*, *6*) but more recent spectroscopic data indicate that the surface complex may be inner-sphere (*4*).

The kinetics of surface chemical reactions are extremely rapid, occurring within milliseconds (*7*). Conventional kinetic techniques (batch and flow methods) are too slow to measure surface chemical reactions. Fortunately, ion adsorption onto metal oxide surfaces can be determined using pressure-jump relaxation kinetics. This technique is based on the fact that the equilibrium constant for a chemical reaction is dependent upon pressure (*8*).

This principle is described by the following expression:

$$\left(\frac{\partial \ln K}{\partial \ln P}\right)_T = -\frac{\Delta V}{RT} \quad (1)$$

where $K$ is the chemical equilibrium constant, $P$ is the pressure, $\Delta V$ is the change in the standard molar volume of the reaction, $R$ is the universal gas constant, and $T$ the absolute temperature. Thus, a pressure perturbation will cause a shift in equilibrium states, and the pressure-jump apparatus is able to monitor the change in conductivity as the system relaxes from an initial to a final equilibrium state. From the relaxation time constants ($\tau$), it is then possible to determine rate constants for surface chemical reactions, but more importantly, pressure-jump relaxation kinetics provide an understanding of reaction mechanisms. However, definitive mechanistic information is obtained only when this technique is used in conjunction with surface spectroscopic probes, e.g., X-ray absorption fine structure (XAFS) spectroscopy. The *p*-jump technique is also valuable because it simultaneously provides information on both adsorption and desorption processes. Numerous studies have used *p*-jump to evaluate the adsorption/desorption of oxyanions on soil constituent surfaces and include the following: adsorption of chromate and phosphate on $\gamma$-$Al_2O_3$ (*9*, *10*), sulfate (*11*), molybdenum (*12*), selenate and selenite (*13*) on goethite (α-FeOOH), and borate on pyrophyllite (*14*). There are no reported *p*-jump studies that have investigated the adsorption/desorption behavior of arsenate and chromate on goethite. Goethite is ubiquitous and the most stable iron oxide in soil environments. It has a well-characterized surface chemistry and morphology and is a major adsorbent in many soils. Hence, studying its interaction with arsenate and chromate will help elucidate the fate of these pollutants in natural systems.

The objectives of this study were to use pressure-jump relaxation kinetics to (i) determine rate constants for the adsorption/desorption of arsenate and chromate on goethite,

* Corresponding author phone: 801-797-0411; fax: 801-797-2117; e-mail address: grossl@cc.usu.edu.
† Utah State University.
‡ Louisiana State University Agricultural Center.
§ University of Delaware.
|| U.S. Salinity Laboratory.
⊥ Battelle, Pacific Northwest Laboratory.

S0013-936X(95)00654-7 CCC: $14.00 

(ii) describe a plausible mechanisms for the adsorption of these oxyanions on goethite using *p*-jump data in conjunction with XAFS spectroscopy information (*4*), and (iii) compare the adsorption behavior of these two oxyanions with one another.

## Materials and Methods

**Sample Preparation.** The samples used for the *p*-jump kinetic studies were from the same batch as samples used for equilibrium adsorption and XAFS studies (*4*). Sample preparation involved equilibrating a given concentration of arsenate or chromate with a specific quantity of goethite at a given pH. Arsenate (as sodium arsenate) at a concentration of 1 mM was equilibrated with a 10 g $L^{-1}$ goethite suspension in the presence of 0.01 and 0.1 M $NaNO_3$, added as background electrolyte. A total of 1 mM chromate (as sodium chromate) was equilibrated with the same quantity of goethite and with 0.001, 0.01, and 0.1 M $NaNO_3$. All reactants were prepared using American Chemical Society reagent-grade chemicals.

The goethite was synthesized from reagent-grade $Fe(NO_3)_3$ using the method described in Schwertmann and Cornell (*15*). Excess salts were washed from the goethite precipitate by electrodialysis until the conductivity of the wash solution was equal to that of distilled-deionized water (~14 days). The clean goethite precipitate was then freeze-dried and stored under desiccation. The identity of the goethite was verified by X-ray diffraction (XRD) analysis and transmission electron microscopy (TEM). The XRD spectra and TEM micrographs were consistent with those for goethite presented in Schwertmann and Connell (15). The surface area of the goethite was equal to 50 $m^2$ $g^{-1}$ determined from a triple-point $N_2$ Brunauer−Emmett−Teller (BET) adsorption isotherm.

The samples used for the *p*-jump, equilibrium adsorption data, and XAFS analysis were prepared in a flat-bottomed, water-jacketed reaction vessel (400 mL) covered with a removable Plexiglas lid containing entry ports for a stirrer, a pH electrode, $N_2$ gas, and burette tip. The goethite suspensions together with the adsorptive and background electrolyte were mixed with an overhead driven polyethylene propeller stirrer spinning at about 5.0 revolutions $s^{-1}$ at a constant temperature of 298.2 ± 0.1 K. After the desired pH was reached, by dropwise addition of either 0.2 M $HNO_3$ or NaOH, 20 mL of the suspension was removed and transferred to 50-mL polypropylene centrifuge tubes that were placed on a reciprocating shaker (180 cycles $min^{-1}$) for 24 h. Afterwards, the pH of the sample was checked for any drift and, if necessary, pH was readjusted to the desired value. Half of the sample (10 mL) was then set aside to be used for p-jump experiments. The remaining 10 mL was centrifuged at 20000*g*, and the supernatant was filtered through 0.2-$\mu$m filters and analyzed for Cr or As by inductively coupled plasma spectrometry. The centrifuge tube containing only the solid was tightly sealed and stored in a refrigerator at 10 °C. The solid was then analyzed using XAFS (*4*).

***p*-Jump Experiments.** A detailed description of the p-jump instrument used for our studies is described in detail by Grossl et al. (*16*). *p*-jump experiments were conducted by filling a sample electrode cell with the suspension equilibrated with the adsorbate at a selected pH. For the arsenate investigations, the pH range for the kinetic experiments was from 6.5 to 8.0, and for the chromate studies, the pH range was from 5.5 to 6.5. To conduct a *p*-jump experiment, it was necessary that during the course of an experiment (~1 h) particle settling was kept to a minimum. Sample suspensions were sonified at least 1 h prior to data collection. The filtered supernatant of the equilibrated suspensions was then added to the reference electrode cell. The cells, sealed with a thin Teflon membrane, were inserted into the pressure autoclave, which comprised one part of the whole pressure-jump apparatus, the other part being a system for conductivity detection.

The entire pressure autoclave was encased in a water jacket. The water jacket was connected to a temperature-controlled water bath that circulated water around the apparatus to maintain a constant temperature. All *p*-jump experiments were conducted at 298.2 ± 0.1 K. The autoclave was sealed with a thin strip of brass foil milled to burst once the pressure within reached approximately 13.5 MPa. Pressure was applied to the autoclave by forcing water into the chamber with a hand-operated mechanical pump. The pressure perturbation was attained by increasing the pressure until the brass foil burst and the pressure instantaneously (~60 ms) dropped to ambient conditions. The sample equilibrated at the higher pressure (13.5 MPa) relaxed to the new equilibrium established at ambient pressure.

The relaxation information was monitored by the conductivity detection system, comprised of a wheatstone bridge, a digitizer, an oscilloscope, and a personal computer containing a data evaluation software program. The sample and reference electrode cells were linked to and comprised two arms of the wheatstone bridge. The other two arms were made up of variable resistors and capacitors that were adjusted to balance the bridge using the oscilloscope as a viewing screen. The bridge was balanced at ambient conditions and became unbalanced upon pressurization. Thus, after the brass foil ruptured, a piezoelectric capacitor triggered collection of the relaxation event, which was recorded as the voltage change associated with the bridge returning to the original balanced state. This information was digitized and relayed to a microcomputer, where the relaxation curve was immediately displayed on the computer monitor. The information was plotted as the relative amplitude of the relaxation as a function of time in seconds, and a software program provided by the manufacturer allowed for quick and direct computation of relaxation time constants or $\tau$ . $\tau$ is the time it takes the relaxation to reach 1/e of the initial amplitude. For each experiment, 12−20 relaxation curves were generated.

To confirm that the relaxation signals were due to the interaction of the adsorbates (arsenate and chromate) with the goethite surface, we conducted *p*-jump experiments with the separate components, i.e., goethite suspensions without adsorbates, and on solutions containing only arsenate and chromate without goethite. No interfering relaxation signals were detected.

**Surface Complexation Modeling.** The constant capacitance model (CCM) (*17*) was used to simulate the adsorption of chromate and arsenate on goethite. This model assumes that reacting ions are specifically adsorbed forming inner-sphere surface complexes and that background electrolyte ions do not interact with the surface-forming complexes. The model also assumes that the net surface charge is a linear function of the surface potential represented by

$$\sigma = (CSa/F)\psi \qquad (2)$$

where $\sigma$ is the surface charge ($mol_c$ $L^{-1}$), $C$ is the capacitance density (F $m^{-2}$), $S$ is the specific surface area ($m^2$ $kg^{-1}$), $a$ is the suspension density of the solid (kg $L^{-1}$), $F$ is the Faraday constant ($9.65 \times 10^{-4}$ C $mol^{-1}$), and $\psi$ is the surface potential (V). We used the CCM to predict the adsorption of chromate and arsenate on goethite as both monodentate and bidentate surface species (Table 1). The capacitance density value used in the CCM calculations was fixed at 1.06 F $m^{-2}$ (*18*), and the surface site density was 2.3 sites $nm^{-2}$, which was determined from arsenate and chromate adsorption isotherms. The arsenate and chromate isotherms were conducted at pH values of 6.8 and 6.0, respectively, and initial concentrations ranging from 0.25 to 3.0 mM. The intrinsic surface acidity

**TABLE 1. Surface Complexation Reactions and Constant Capacitance Model (CCM) Intrinsic Surface Complexation Constants Used in This Study**

| reactions | equilibrium expressions and constants |
|---|---|
| **Surface Hydrolysis Reactions** | |
| (1) $XOH + H^+ = XOH_2^+$ [a] | $K_{a1}(\text{int}) = \frac{[XOH_2^+]}{[XOH][H^+]} \exp\left(\frac{F\psi}{RT}\right) = 10^{7.31}$ [b] |
| (2) $XOH = XO^- + H^+$ | $K_{a2}(\text{int}) = \frac{[XO^-][H^+]}{[XOH]} \exp\left(-\frac{F\psi}{RT}\right) = 10^{-8.81}$ [b] |
| **Formation of Inner-Sphere Monodentate Oxyanion/Goethite Surface Complexes** | |
| (3) $XOH + H_3AsO_4 = XH_2AsO_4 + H_2O$ | $K^1_{As}(\text{int}) = \frac{[XH_2AsO_4]}{[XOH][H_3AsO_4]} = 10^{10}$ |
| (4) $XOH + H_3AsO_4 = XHAsO_4^- + H_2O + H^+$ | $K^2_{As}(\text{int}) = \frac{[XHAsO_4^-][H^+]}{[XOH][H_3AsO_4]} \exp\left(-\frac{F\psi}{RT}\right) = 10^{5.1}$ |
| (5) $XOH + H_3AsO_4 = XHAsO_4^{2-} + H_2O + 2H^+$ | $K^3_{As}(\text{int}) = \frac{[XAsO_4^{2-}][H^+]^2}{[XOH][H_3AsO_4]} \exp\left(-\frac{F\psi}{RT}\right) = 10^{0.55}$ |
| (6) $XOH + H_2CrO_4 = XHCrO_4 + H_2O$ | $K^1_{Cr}(\text{int}) = \frac{[XHCrO_4]}{[XOH][H_2CrO_4]} = 10^{9.8}$ |
| (7) $XOH + H_2CrO_4 = XCrO_4^- + H_2O + H^+$ | $K^2_{Cr}(\text{int}) = \frac{[XCrO_4^-][H^+]}{[XOH][H_2CrO_4]} \exp\left(-\frac{F\psi}{RT}\right) = 10^{4.2}$ |
| **Formation of Inner-Sphere Bidentate Oxyanion/Goethite Surface Complexes** | |
| (8) $2XOH + H_3AsO_4 = X_2HAsO_4 + 2H_2O$ | $K^4_{As}(\text{int}) = \frac{[X_2HAsO_4]}{[XOH]^2[H_3AsO_4]} = 10^{17}$ |
| (9) $2XOH + H_3AsO_4 = X_2AsO_4^- + 2H_2O + H^+$ | $K^5_{As}(\text{int}) = \frac{[X_2AsO_4^-][H^+]}{[XOH]^2[H_3AsO_4]} \exp\left(-\frac{F\psi}{RT}\right) = 10^{11.4}$ |
| (10) $2XOH + H_2CrO_4 = X_2CrO_4 + 2H_2O$ | $K^3_{Cr}(\text{int}) = \frac{[X_2CrO_4]}{[XOH]^2[H_2CrO_4]} = 10^{15.3}$ |

[a] X symbolizes the goethite surface. [b] From Goldberg (*1*).

constants were $10^{7.31}$ and $10^{-8.80}$ for $K_{a1}$ and $K_{a2}$, respectively (*1*). These values are averages from a literature compilation of experimental data (*18*). The least square optimization program, FITEQL Version 3.1 (*19*), was used to fit intrinsic surface complexation constants (Table 1) to the experimental equilibrium adsorption data and to compute the concentrations of surface complexes. The acid dissociation constants used in the CCM were $K_{a1} = 10^{-2.24}$, $K_{a2} = 10^{-6.94}$, and $K_{a3} = 10^{-11.50}$ for arsenic acid and $K_{a1} = 10^{0.20}$ and $K_{a2} = 10^{-6.51}$ for chromic acid (*20*).

## Results and Discussion

**Equilibrium Adsorption Study.** The quantity of arsenate and chromate adsorbed on goethite as a function of pH is displayed in Figures 1 and 2. The adsorption envelope for arsenate (Figure 1) was much broader than that for chromate (Figure 2). The differences in adsorption edges between oxyanions can be related to the degree of protonation of the molecule. Arsenate is a triprotic acid while chromate is a diprotic acid. Triprotic acids will exhibit a much broader adsorption edge over a wide pH range than a diprotic acid, which displays a steeper adsorption edge. This is because the adsorption of weak acids is strongest at pH values near their acid dissociation constants (*21*). These results are consistent with other equilibrium studies investigating oxyanion adsorption on goethite (*1*, *22*). There was no difference between adsorption edges for either arsenate and chromate measured at varying background electrolyte concentrations (Figures 1 and 2). This suggests that both oxyanions form inner-sphere surface complexes with goethite. Recent X-ray absorption fine structure (XAFS) spectroscopic studies (*2*–*4*) indicate that these oxyanions form inner-sphere bidentate

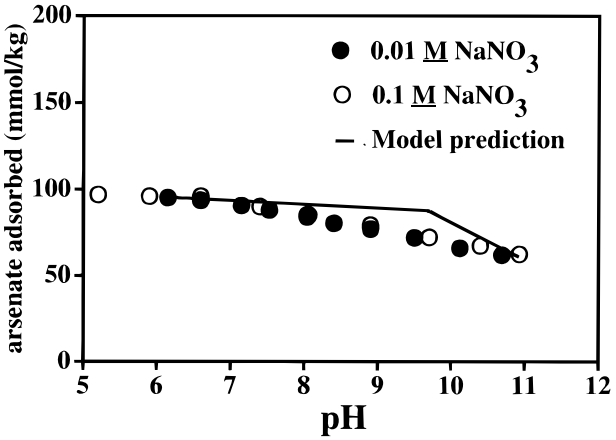


**FIGURE 1. Equilibrium adsorption data for arsenate adsorption on goethite versus pH. Values in legend indicate background electrolyte ($NaNO_3$) concentrations.**

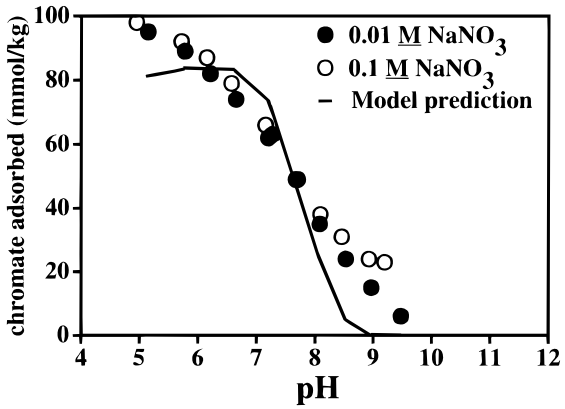


**FIGURE 2. Equilibrium adsorption data for chromate adsorption on goethite versus pH. Values in legend indicate background electrolyte ($NaNO_3$) concentrations.**

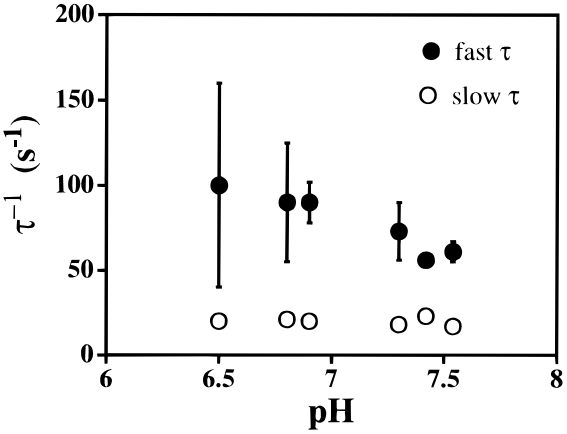


**FIGURE 3. $\tau^{-1}$ values determined from *p*-jump experiments for arsenate adsorption/desorption on goethite, as a function of pH.**

surface complexes with goethite. Hence, we used the CCM to simulate chromate and arsenate adsorption as an inner-sphere bidentate surface complex. The simulations fit the experimental data reasonably well (Figures 1 and 2), indicated by the values of the weighted sum of squares divided by degrees of freedom (WSOS/DF). Commonly, WSOS/DF values less than 20 denote a reasonably good fit (*19*), which was the case for our simulations. The WSOS/DF value for the model prediction in Figure 1 was 17.6, and the value was 18.9 for the prediction in Figure 2. The intrinsic equilibrium constants calculated for the surface reactions are listed in Table 1.

**Kinetic Study.** The pressure-jump technique was used to (i) help elucidate the adsorption mechanism proposed from the equilibrium studies and (ii) to provide rate constants for both adsorption and desorption reactions. Pressure-jump relaxation experiments were evaluated for arsenate and chromate over the pH ranges 6.5−7.5 and 5.5−6.5, respectively. Additionally, *p*-jump experiments were conducted on samples simultaneously used to develop isotherms for the adsorption of arsenate and chromate on goethite. The initial concentrations of these oxyanions in the samples ranged from 0.5 to 2.0 mM. In these pH and concentration ranges, we were able to confidently associate the relaxation signals with the adsorption/desorption of both oxyanions. A double relaxation event was observed for both arsenate and chromate adsorption/desorption on goethite (Figures 3 and 4). For the pH experiments with both oxyanions, the slow $\tau$ values remained constant at about 50 ms. However, for arsenate, the faster $\tau$ values increased with increasing pH from about 10 to 20 ms and from 2.5 to 10 ms for chromate (Figures 3 and 4). A similar trend between fast and slow $\tau$ values was

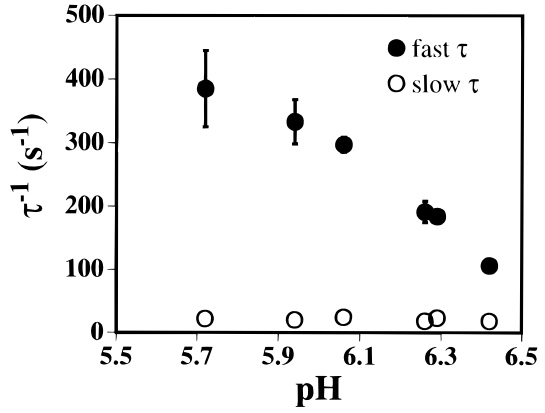


**FIGURE 4. $\tau^{-1}$ values determined from *p*-jump experiments for chromate adsorption/desorption on goethite, as a function of pH.**

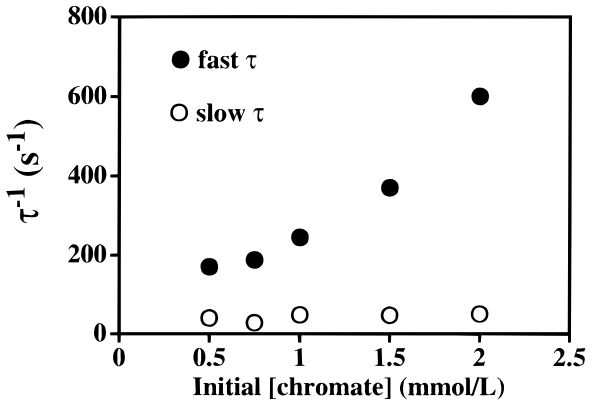


**FIGURE 5. $\tau^{-1}$ values determined from *p*-jump experiments for chromate adsorption/desorption on goethite, as a function of initial chromate concentration. Adsorption/desorption of arsenate on goethite as a function of initial arsenate levels followed a similar trend.**

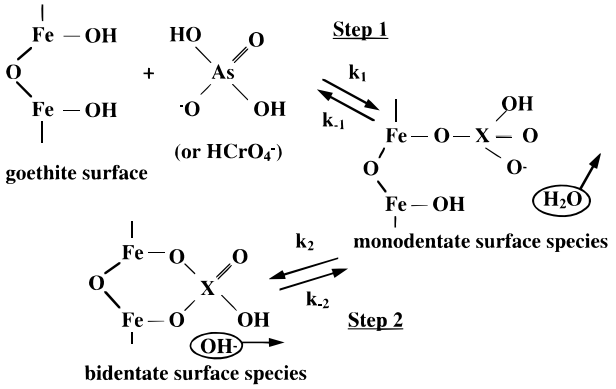


**FIGURE 6. Proposed mechanism for oxyanion adsorption/desorption on goethite. The X represents either As(V) or Cr(VI).**

observed for adsorption isotherm samples that were evaluated using *p*-jump (Figure 5).

We propose that the mechanism for oxyanion adsorption on goethite is a two-step process resulting in the formation of an inner-sphere bidentate surface complex (Figure 6). The first step involves an initial ligand exchange reaction of the aqueous oxyanion ($H_2AsO_4^-$ or $HCrO_4^-$) with goethite, forming an inner-sphere monodentate surface complex. This first step produces the signals associated with the fast $\tau$ values. The succeeding step involves a second ligand exchange reaction, resulting in the formation of an inner-sphere bidentate surface complex. This step produces the signal associated with the slow $\tau$ values.

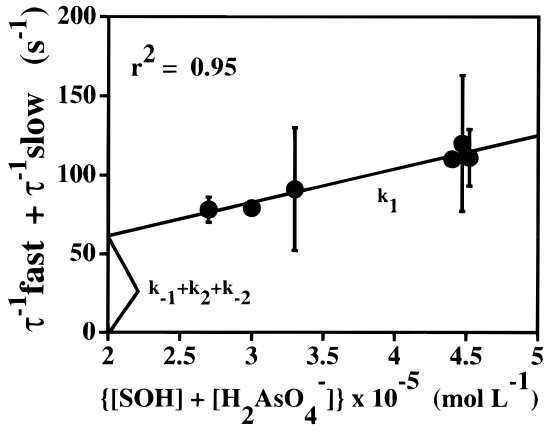


**FIGURE 7. Evaluation of the linearized rate equation (eq 3) for the mechanism displayed in Figure 6 for arsenate.**

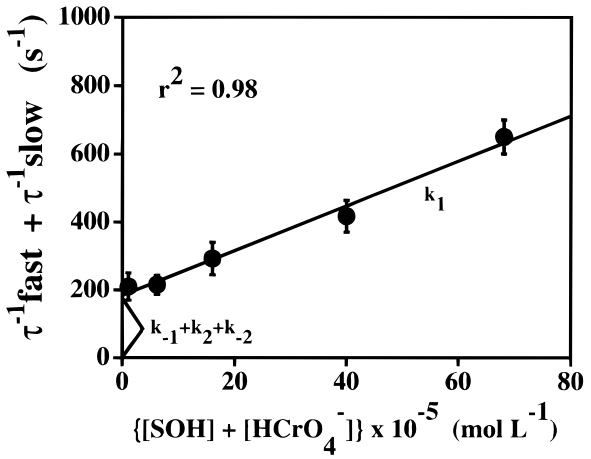


**FIGURE 8. Evaluation of the linearized rate equation (eq 3) for the mechanism displayed in Figure 6 for chromate.**

To determine if the mechanism displayed in Figure 6 was plausible and consistent with our kinetic data, the following linearized rate equations relating $\tau^{-1}$ values to the concentrations of reactive species were used:

$$\tau_{\text{fast}}^{-1} + \tau_{\text{slow}}^{-1} = k_1([\text{XOH}] + [\text{ion species}]) + k_{-1} + k_2 + k_{-2} \quad (3)$$

$$\tau^{-1}{}_{\text{fast}} \times \tau^{-1}{}_{\text{slow}} = k_1[k_2 + k_{-2}]\{[\text{XOH}] + [\text{ion species}]\} + k_{-1}k_{-2} \quad (4)$$

where the ion species are $H_2AsO_4^-$ or $HCrO_4^-$. The derivation of these equations was obtained from Bernasconi (*8*) and is based on the two-step reaction system (A + B ↔ C ↔ D). If the mechanism portrayed in Figure 6 is accurate, then a plot of $\tau_f^{-1} + \tau_s^{-1}$ and $\tau_f^{-1} \times \tau_s^{-1}$ as a function of the concentration term ([XOH] + [ion species]) should be linear. Plots of eqs 3 and 4 were linear, suggesting that the proposed mechanism was plausible (Figures 7−10).

From these plots, forward and reverse rate constants were obtained for the adsorption and desorption reactions of both the monodentate and bidentate steps, where $k_1$ was the slope of lines plotted in Figures 7 and 8; $k_{-1}$ was the *y*-intercept of the lines plotted in Figures 7 and 8 minus the ratio of the respective slopes of the lines plotted in Figures 9 and 10 divided by the respective slopes of the lines plotted in Figures 7 and 8; $k_{-2}$ was the *y*-intercept of the lines plotted in Figures 9 and 10 divided by the respective values of $k_{-1}$; and $k_2$ was the *y*-intercept of the lines plotted in Figures 7 and 8 minus both the respective $k_{-1}$ and $k_{-2}$ values. The calculated rate constants for both chromate and arsenate adsorption/desorption on goethite are listed in Table 2. Overall, the forward rate constants associated with the formation of the inner-sphere oxyanion/goethite surface complexes were more rapid than the reverse rate constants. The equilibrium constants listed in Table 2 were calculated from the rate constants for each reaction step of the proposed mechanism (Figure 6) at 298.2 K using the following relationship:

$$K_{\text{eq}} = k_{\text{forward}}/k_{\text{reverse}} \quad (5)$$

This relationship establishes the fundamental link between thermodynamics and kinetics (*7*). The calculated equilibrium constant for step 1 for arsenate was $10^{5.35}$ and for step 2 was $10^{0.26}$, while the calculated $K_{eq}$ for step 1 for chromate was $10^{3.7}$ and for step 2 was $10^{-0.4}$. Based on these kinetically determined equilibrium constants, we surmise that the reaction depicted in Figure 6 favors products (inner-sphere surface complexes). Only the second step associated with chromate adsorption had a calculated equilibrium constant slightly less than 1. Thus, the monodentate chromate/goethite surface complex is slightly favored over the bidentate

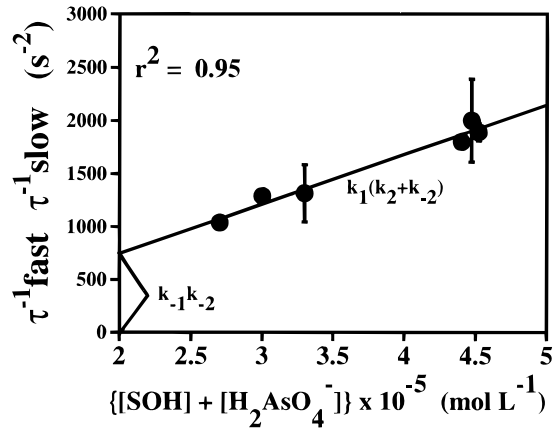


**FIGURE 9. Evaluation of the linearized rate equation (eq 4) for the mechanism displayed in Figure 6 for arsenate.**

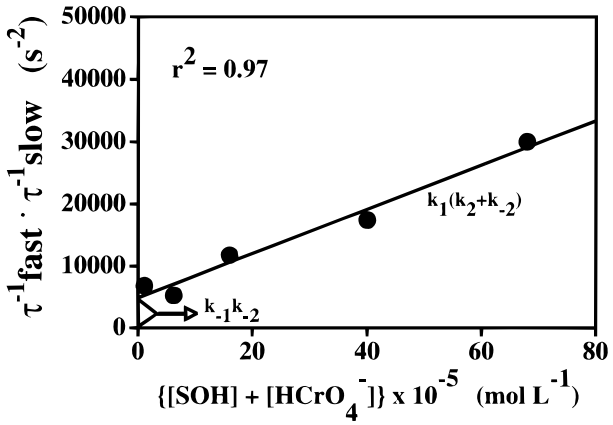


**FIGURE 10. Evaluation of the linearized rate equation (eq 4) for the mechanism displayed in Figure 6 for chromate.**

**TABLE 2. Calculated Rate Constants for Chromate and Arsenate Adsorption/Desorption on Goethite**

| | step 1 | step 2 |
|---|---|---|
| arsenate | $k_1 = 10^{6.3}$ L mol$^{-1}$ s$^{-1}$<br>$k_{-1} = 8$ s$^{-1}$<br>$K_{eq} = 10^{5.35}$ L mol$^{-1}$ | $k_2 = 15$ s$^{-1}$<br>$k_{-2} = 8$ s$^{-1}$<br>$K_{eq} = 10^{0.26}$ |
| chromate | $k_1 = 10^{5.8}$ L mol$^{-1}$ s$^{-1}$<br>$k_{-1} = 129$ s$^{-1}$<br>$K_{eq} = 10^{3.7}$ L mol$^{-1}$ | $k_2 = 16$ s$^{-1}$<br>$k_{-2} = 38$ s$^{-1}$<br>$K_{eq} = 10^{-0.4}$ |

surface complex. This agrees with spectroscopic data (XAFS), which indicates a mixture of both monodentate and bidentate arsenate and chromate surface complexes, but at low surface coverage a greater proportion of chromate is associated with the monodentate complex than the bidentate complex (*4*). The results from both kinetic and equilibrium batch experiments suggest that arsenate is more likely to form an inner-sphere surface complex with goethite than chromate. Consequently, arsenate might be more readily adsorbed in soil systems, and chromate may be the more mobile of the two oxyanions in natural systems. This is in agreement with results of Zachara et al. (*6*) and Stollenwerk and Grove (*23*), who found chromate to be fairly mobile in soil environments.

The kinetically determined equilibrium constants for the overall formation of the bidentate oxyanion/goethite surface complexes $\{K_{eq(step\ 1)} \times K_{eq(step\ 2)}\}$ (Table 2) were much smaller than the intrinsic $K$ values for reactions 8 and 10 in Table 1, which were calculated using the CCM. However, the kinetically determined values for the formation of the monodentate surface complexes (step 1) were consistent with $K_{int}$ values for the same reaction calculated with the CCM (*1*). This suggests that the mechanism proposed for step 1 is valid, but step 2 may involve more elementary reactions than are illustrated in Figure 7, thus increasing the overall value of the equilibrium constant. It is possible that a bidentate-mononuclear complex contributes to this adsorption step as well. This is a reasonable assumption since the *p*-jump apparatus can monitor only reactions that generate measurable changes in conductivity. If step 2 involved other elementary surface reactions that could not be detected using *p*-jump, our proposed mechanism (Figure 6) may not be complete. Advanced spectroscopic and microscopic surface probes may resolve this issue in the future. Regardless, kinetic, equilibrium adsorption, and spectroscopic evidence (*2*−*4*) indicate that arsenate forms an inner-sphere bidentate surface complex with goethite, while chromate forms a combination of monodentate and bidentate surface complexes with goethite.

## Acknowledgments

We gratefully acknowledge Dr. George Luther III for his insightful comments. We are also grateful to the Utah Agricultural Experiment Station for its support.

## Literature Cited

(1) Goldberg, S. *Soil Sci. Soc. Am. J.* **1986**, *50*, 1154−1157.
(2) Waychunas, G. A.; Rea, B. A.; Fuller, C. C.; Davis, J. A. *Geochim. Cosmochim. Acta* **1993**, *57*, 2251−2269.
(3) Waychunas, G. A.; Fuller, C. C.; Rea, B. A.; Davis, J. A. *Geochim. Cosmochim. Acta* **1996**, *60*, 1765−1781.
(4) Fendorf, S. E.; Eick, M. J.; Grossl, P. R.; Sparks, D. L. *Environ. Sci. Technol.* **1997**, *31*, 315−320.
(5) Hayes, K. F. Ph.D. Dissertation, Stanford University, 1987.
(6) Zachara, J. M.; Cowan, C. E.; Schmidt R. L.; Ainsworth, C. C. *Clays Clay Miner.* **1988**, *36*, 317−326.
(7) Amacher, M. C. In *Rates of Soil Chemical Processes;* Sparks, D. L., Suarez, D. L., Eds.; Special Publication 27; Soil Science Society of America: Madison, WI; 1991; pp 19−59.
(8) Bernasconi, C. F. *Relaxation Kinetics*; Academic Press: New York, 1976.
(9) Mikami, N.; Sasaki, M.; Kikuchi, T.; Yasunaga, T. *J. Phys. Chem.* **1983**, *87*, 5245−5248.
(10) Mikami, N.; Sasaki, M.; Hachiya,K.; Astumian, R. D.; Ikeda, T.; Yasunaga, T. *J. Phys. Chem.* **1983**, *87*, 1454−1458.
(11) Zhang, P. C.; Sparks, D. L. *Soil Sci. Soc. Am. J.* **1990**, *54*, 1266−1273.
(12) Zhang, P. C.; Sparks, D. L. *Soil Sci. Soc. Am. J.* **1989**, *53*, 1028−1034.
(13) Zhang, P. C.; Sparks, D. L. *Environ. Sci. Technol.* **1990**, *24*, 1848−1856.
(14) Keren, R; Grossl, P. R.; Sparks, D. L. *Soil Sci. Soc. Am. J.* **1994**, *58*, 1116−1122.
(15) Schwertmann, U.; Cornell, R. M. *Iron oxides in the laboratory. Preparation and characterization;* VCH: New York, 1991; Chapter 5.
(16) Grossl, P. R.; Sparks, D. L.; Ainsworth, C. C. *Environ. Sci. Technol.* **1994**, *28*, 1422−1429.
(17) Stumm, W. R.; Kummert, R.; Sigg, L. *Croat. Chem. Acta*. **1980**, *53*, 291−312.
(18) Goldberg, S.; Sposito, G. *Soil Sci. Soc. Am. J.* **1984**, *48*, 772−778.
(19) Herbelin, A. L.; Westall, J. C. *FITEQL 3.1*; Oregon State University: Corvallis, OR, 1994.
(20) Martell, A. E.; Smith, R. M. *Critical Stability Constants*; Plenum Press: New York, 1974.
(21) Hingston, F. J.; Posner, A. M.; Quirk, J. P. *J. Soil Sci*. **1972**, *23*, 177−192.
(22) Hingston, F. J.; Posner, A. M.; Quirk, J. P. *Discuss. Faraday Soc.* **1971**, *52*, 334-342.
(23) Stollenwerk, K. G.; Grove, D. B. *J. Environ. Qual*. **1985**, *14*, 150−155.

*Received for review September 6, 1995. Revised manuscript received September 11, 1996. Accepted September 11, 1996.*[⊗]

ES950654L

[⊗] Abstract published in *Advance ACS Abstracts,* November 15, 1996.